

Transition to Centrifugal Particle Motion in Rotating Drums

Gerald H. Ristow

*Fachbereich Physik, Philipps-Universität
Renthof 6, D-35032 Marburg, Germany*

(received June 3, 1998; revised June 22, 1998)

Abstract

The dynamics and the transition to the centrifugal regime are studied analytically and numerically for particles in rotating drum. The importance of the particle-wall friction coefficient is demonstrated by studying first the motion of one non-rotating particle where three different regimes are found in the transition to the centrifugal motion. When a few rotating particles are considered, they behave similarly to one non-rotating particle in the low friction limit. A critical particle number is necessary to reach the centrifugal regime for which an analytic expression is derived in the limit of negligible inter-particle friction.

PACS: 81.05.Rm, 46.30.Pa, 05.70.Fh, (46.10+z)

1 Introduction

Granular materials can show fascinating behaviour in many experimental situations [1]. When placed in a slowly rotating drum, most particles undergo a solid body rotation by following the external motion and a thin layer of intermittently flowing particles (avalanches) is forming close to the surface. With increasing rotation speed, the separation time of avalanches will decrease until no individual avalanches are detectable and a nearly constant particle flow is found along the free surface [2]. For even higher rotation speeds, the free surface does not stay flat but rather deforms with increasing rotation speed. These deformations mostly start from the lower boundary inwards [3]. When the rotation speed is further increased, the particle motion is dominated by the centrifugal force leading to a ring formation close to the outer wall boundary [4]. In order to understand the different flowing regimes, it is instructive to study the particle dynamics on a microscopic level, i.e. on a particle basis. This is especially helpful for studying different frictional forces [5] which play an important role in many other technological problems

as well [6]. In a simplified view, one can look at the particles undergoing a solid body rotation as sticking to their neighbours whereas the particles in the fluidized surface layer undergo mostly sliding collisions. A similar particle behaviour can be observed for a particle placed on a moving plate and attached to one side wall via a spring. For low surface velocities, a stick-slip motion is observed and above a critical velocity, the stick-slip motion disappears and only steady sliding is observed [7, 8]. But this setup might not allow for long enough observation times in order to investigate transient behaviour. We propose another setup, namely to place the particle(s) in a rotating drum.

The paper is organized in the following way: in section 2, we will sketch the system in mind, explain briefly an experimental realization and derive the equation of motion for one non-rotating particle in the full-sliding limit. In section 3, we will present a numerical model which is not restricted to the full-sliding limit but is capable to explore the full particle dynamics including the transition from sticking to sliding motion. This will be compared in section 4 to the analytic solution and the transition to the *centrifugal regime* will be discussed. In section 5, the collective behaviour of a few rotating spheres in the drum will be investigated and a connection to the one particle case can be made. The conclusions will round off this paper.

2 Setup and Theory for One Non-Rotating Particle

Different friction regimes for particle-wall contacts can be studied by looking at the dynamics of a non-rotating particle placed in a rotating drum. The setup is sketched in Fig. 1a where the particle is approximated by a sphere shown in grey. The drum rotates with a constant angular velocity Ω , gravity is pointing downwards and the angle φ of the particle's center of mass is measured from the vertical. The distance between the drum's and the particle's center is R . In the corresponding experimental system, the non-rotating particle was realized by glueing two spheres together and the drum was slightly tilted in order to force the particle to slide along one of the end caps [9].

The equation of motion is one-dimensional as long as the particle stays in contact with the wall of the drum, i.e. $R \equiv \text{constant}$. For full sliding, $|\dot{\varphi}| < \Omega$, the equation of motion reads

$$\begin{aligned} \frac{F}{m} = R\ddot{\varphi} &= -\underbrace{g \sin \varphi}_{F_s} + \mu_w \underbrace{(g \cos \varphi + R\dot{\varphi}^2)}_{F_n} \\ &= -g \sqrt{1 + \mu_w^2} \sin(\varphi - \varphi_0) + \mu_w R\dot{\varphi}^2 \end{aligned} \tag{1}$$

where $\varphi_0 \equiv \arctan(\mu_w)$ and the Coulomb friction law was used. Here F_n denotes the normal force and F_s the shear force. Having the many particle program at hand, we

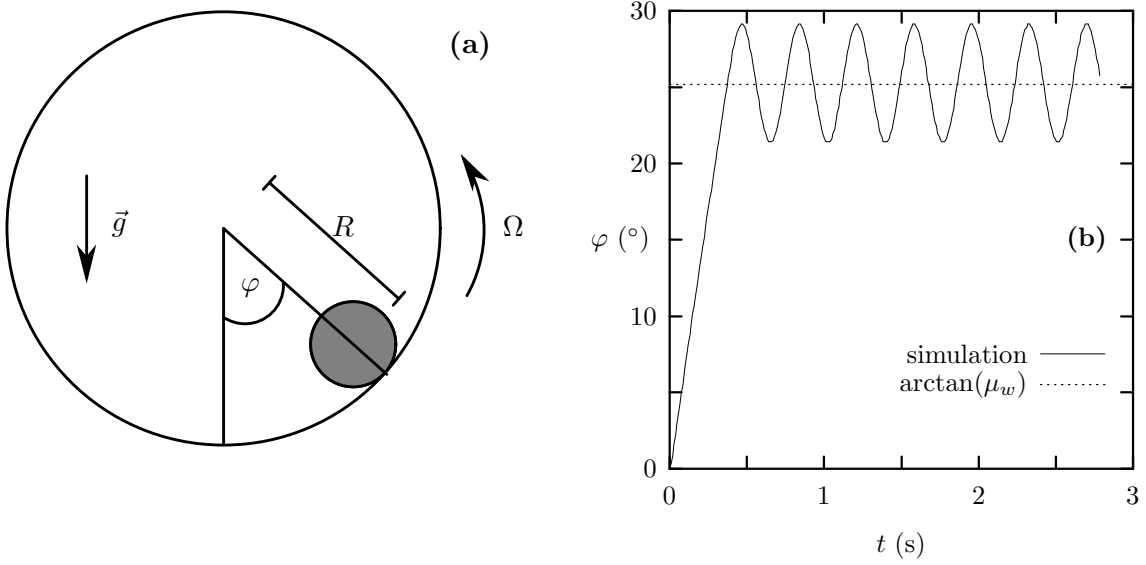


Figure 1: (a) Sketch of the quasi one-dimensional setup and (b) evolution of the angle as function of time in the simulation for $\mu_w = 0.47$.

used MD simulations and compared the results for one non-rotating particle with the experiment and the theory. The angle φ as function of time for a typical run is shown in Fig. 1b using a drum rotation speed of $\Omega = 1$ Hz and the initial conditions $\varphi(0) = \dot{\varphi}(0) = 0$.

Equation (1) can be simplified by the following steps [10]: setting $\tilde{\varphi} \equiv \varphi - \varphi_0$ one gets

$$R\ddot{\tilde{\varphi}} = -g\sqrt{1 + \mu_w^2} \sin(\tilde{\varphi}) + \mu_w R\dot{\tilde{\varphi}}^2. \quad (2)$$

This equation does not exhibit an explicit time dependence and it is favourable to use the transformation $u(\tilde{\varphi}) \equiv \dot{\tilde{\varphi}} \Rightarrow \ddot{\tilde{\varphi}} = u'\dot{\tilde{\varphi}} = u'u$ leading to the equation

$$Ru'u = -g\sqrt{1 + \mu_w^2} \sin(\tilde{\varphi}) + \mu_w Ru^2. \quad (3)$$

By using the transformation $v \equiv \frac{1}{2}u^2$ the equation can be integrated and one obtains

$$e^{-2\mu_w\tilde{\varphi}}v(\tilde{\varphi}) = -\frac{g\sqrt{1 + \mu_w^2}}{R} \int_{-\varphi_0}^{\tilde{\varphi}} e^{-2\mu_w\Psi} \sin \Psi d\Psi + e^{2\mu_w\varphi} v(-\varphi_0). \quad (4)$$

Please note that the second term on the r.h.s. vanishes for $\dot{\tilde{\varphi}}(t=0) = 0$.

Backtransformation yields the following final equation for $\dot{\varphi}$

$$\dot{\varphi}^2(t) = \frac{2g}{R(1 + 4\mu_w^2)} [3\mu_w \sin \varphi + (1 - 2\mu_w^2) (\cos \varphi - e^{2\mu_w\varphi})] + e^{2\mu_w\varphi} \dot{\varphi}^2(0). \quad (5)$$

It can be integrated numerically by separation of variable but the general class of the motion can already be seen by a stability analysis. By setting $\dot{\varphi} = \ddot{\varphi} = 0$ in the original equation (1) one sees that the fixpoint must fulfill the condition

$$\frac{\sin \varphi}{\cos \varphi} = \tan \varphi = \mu_w$$

which is nothing but the initial definition for φ_0 . To study the stability of the obtained fixpoint, one sets $\varphi(t) = \varphi_0 + \varepsilon(t)$ in Eq. (1) and neglects higher terms in ε and $\dot{\varepsilon}$. The equation of motion for ε reads

$$\ddot{\varepsilon} = -\frac{g}{R \cos \varphi_0} \varepsilon .$$

This states that the fixpoint is marginally stable and the general motion is an oscillation around it of the form

$$\varphi(t) = \varphi_0 + A e^{i\omega t} + B e^{-i\omega t} \quad (6)$$

where

$$\omega := \sqrt{\frac{g}{R \cos \varphi_0}} .$$

This oscillation can be seen in the simulation result shown in Fig. 1b. It is also found for the motion of a particle on a plate [8]. Please note that the frequency of the oscillation in Eq. (6) does not depend on the external angular velocity, Ω , as long as the full-sliding condition is fulfilled.

3 Numerical Model

In order to study the full dynamics of particles in a rotating drum, we use two-dimensional molecular dynamics (MD) simulations. Particles are approximated by spheres and only contact forces during collisions are considered [11]. We use a *linear spring-dashpot model* for the force in normal direction, reading

$$F_n = -k_n h - \gamma_n \dot{h} \quad (7)$$

and a viscous shear force in tangential direction, reading

$$F_s = -\text{sign}(\gamma_s v_{\text{rel}}) \min(\gamma_s |v_{\text{rel}}|, \mu |F_n|) . \quad (8)$$

Here h stands for the virtual overlap of the particle with the wall or with another particle, μ denotes the friction coefficient and v_{rel} the relative velocity of the two surfaces. The Coulomb friction law states that the magnitude of the shear force can at most have a value equal to the magnitude of the normal force multiplied by the friction coefficient. The model parameter k_n is related to the material stiffness, γ_n to the normal restitution

coefficient, e_n , and γ_s is chosen high enough to ensure that mostly the Coulomb friction law applies.

Using MD simulations, the angle φ as function of time for a typical run is shown in Fig. 1b using the parameters $\Omega = 1$ Hz, $e_n = 0.9$ and a particle-wall friction coefficient of $\mu_w = 0.47$ with the initial condition $\varphi(0) = \dot{\varphi}(0) = 0$. The oscillatory motion given by the analytic result, Eq. (6), can be seen as well.

4 Results and Discussion

In order to determine the maximum amplitude of this motion, $\Delta\varphi$, one calculates the second turning point of the motion by setting $\dot{\varphi} = 0$ in Eq. (5) and using the initial conditions $\varphi(0) = 0$ and $\dot{\varphi}(0) = 0$. One obtains

$$\sin \Delta\varphi = \frac{1 - 2\mu_w^2}{3\mu_w} (e^{2\mu_w\Delta\varphi} - \cos \Delta\varphi) , \quad \Delta\varphi > 0 . \quad (9)$$

The sin-function on the l.h.s. can take only values from -1 to +1 and the expression in parentheses on the r.h.s. is always greater than zero which gives for small values of μ_w a solution close to zero. The fraction on the r.h.s. changes sign at $\mu_w = 1/\sqrt{2} \approx 0.7071$ leading to a diverging solution around this value, e.g. for $\mu_w = 0.71$, Eq. (9) does not have a solution. For a more quantitative analysis, the equation was integrated numerically using MATHEMATICA and the obtained solution is shown as solid line in Fig. 2a as function of the friction coefficient μ_w . Even though solutions of $\Delta\varphi > 90^\circ$ are possible analytically from Eq. (9), they do not lead to an oscillating motion since for $\varphi > 90^\circ$ the particle will detach from the wall on its way downwards which invalidates the assumptions leading to Eq. (1). We added in Fig. 2a the data for $\Delta\varphi$ from the MD simulations as open circles (\circ). These were obtained by measuring the angle difference via the maxima and minima in plots like the one shown in Fig. 1b. The values vary very little in time and the agreement with the analytic expression, taken from Eq. (9), is perfect, thus demonstrating that the simulation indeed describes the full-sliding regime when a viscous shear force is used together with the Coulomb threshold criterion, Eq. (8). For angles φ greater than 90 degrees, i.e. points lying above the dotted line in Fig. 2a, the value of $\Delta\varphi$ was obtained by taking the maximum value during the first oscillation just before the free fall during the downwards motion sets in.

The maximum amplitude is only reached for a high enough value of the rotation speed of the drum, Ω , for the chosen initial conditions. For lower values of Ω , the system will oscillate with an intermediate amplitude since they are all marginally stable. If the initial conditions are chosen such that the initial amplitude is greater than $\Delta\varphi$, the system will dissipate energy and finally reach a state with an amplitude lower than or equal to $\Delta\varphi$. In the numerical simulations, the frequency of the oscillation shows no

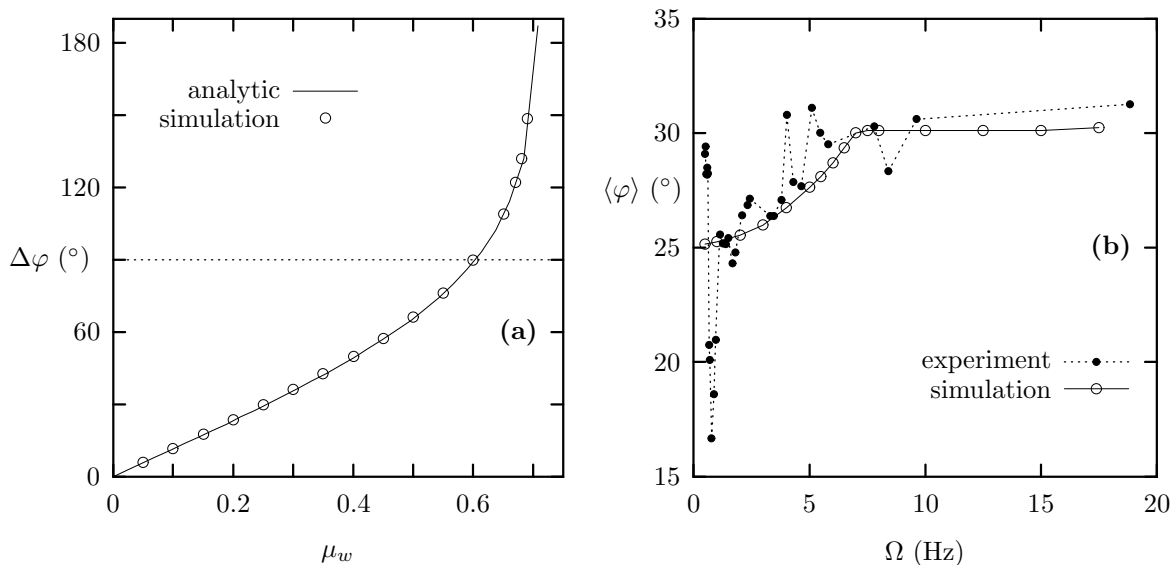


Figure 2: (a) Comparison of the analytic expression for the maximum amplitude with the simulation and (b) frequency dependence of the average angle for the experiment (\bullet) and the simulation using $\mu_w = 0.47$ (\circ).

dependence on the rotation speed Ω in agreement with the analytic result, Eq. (6), as long as the full-sliding condition is fulfilled. The frequency is 16.5 Hz for the simulation, extracted from Fig. 1b, and 16.9 Hz for the analytic expression, Eq. (6). A similar system was investigated experimentally [9] by gluing two spheres together and slightly tilting the drum in order to force the particle to slide along one of the end caps. There, only a weak frequency dependence was found for values of $\Omega > 2.5$ Hz giving a dominant oscillation frequency of 15.7 Hz, but for lower values, a stick-slip motion was clearly visible and led to lower values of the dominant frequency mode in the oscillation. Since no sticking was considered in the analytic model, it cannot capture this feature. The numerical model assumes a perfectly shaped drum whereas in the experiment a slight asphericity was observed and additional friction with one end cap was present thus amplifying the stick-slip region. Keeping these differences in mind the agreement is very satisfactory. By looking at the mean angle, $\langle\varphi\rangle$, of the particle as function of Ω , a similar frequency dependence was found in the experiment. To a certain extent, this is also visible in the MD simulations and we show in Fig. 2b the experimental points, taken from [9], as filled circles (\bullet) and the numerical data by open circles (\circ). For $\Omega \lesssim 7$ Hz, the mean angle decreases with decreasing angular frequency of the drum and the general trend is well captured by the simulation. The large fluctuations in the experimental data can probably be attributed to the stick-slip motion which was enhanced by a slight asphericity of the drum. The best agreement with the experimental data in the high angular frequency

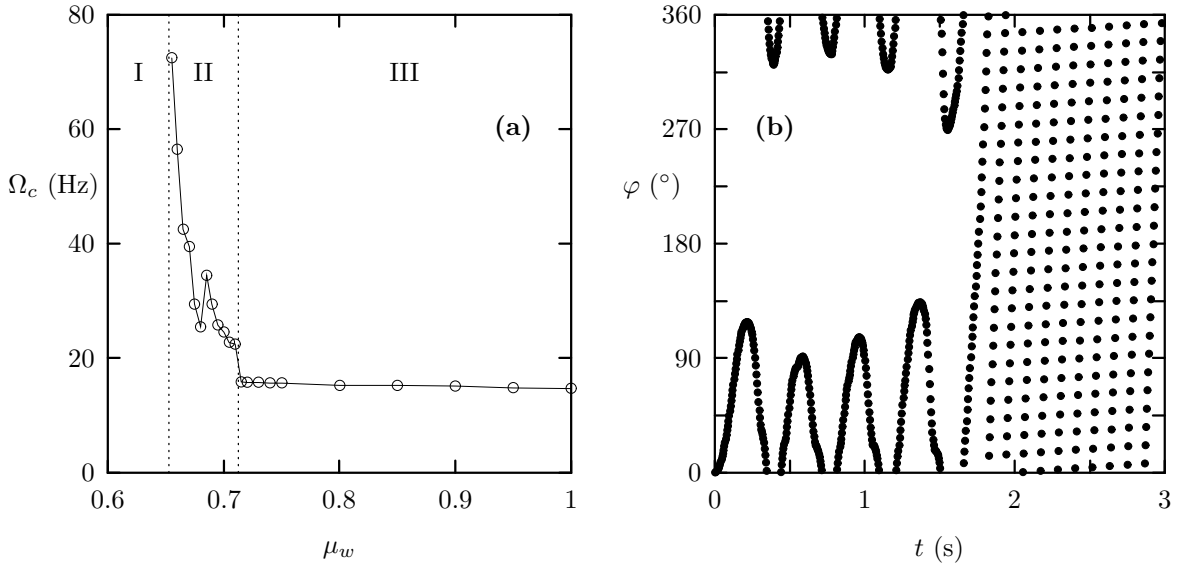


Figure 3: (a) Transition frequency to the centrifugal regime as function of friction coefficient and (b) angle of the particle as function of time for $\mu_w = 0.665$ and $\Omega = 43$ Hz (regime II).

regime was obtained for $\mu_w = 0.47$.

The solution of the analytic Eq. (9) and the corresponding Fig. 2a state that the amplitude of the oscillation will be larger than 180° ($\hat{=} \pi$) for values of $\mu \gtrsim 0.7$ for a sufficiently high value of Ω . Physically that means that the particle will make overturns following the external sense of rotation and touches the wall all the time. This regime will be called the *centrifugal regime* and marked by the symbol III. It exists a well defined transition frequency which we will call Ω_c . The question now arises under what conditions this centrifugal regime exists and if it will be possible to make immediate overturns starting with a particle at rest. To address this question, we investigated numerically the transition frequency, Ω_c , as function of friction coefficient, μ , for a particle initially at rest. It can be viewed as a phase diagram and is shown in Fig. 3a. Three different regimes can be identified: (I) regardless of the angular frequency and the initial conditions the final state will oscillate below an angle of 90 degrees showing no overturns. (II) above a threshold of $\mu \approx 0.65$, the centrifugal regime can be reached and the transition frequency decreases with increasing value of μ . Since the dynamics depends on the initial state, fluctuations in Ω_c are visible. To illustrate this point, we show in Fig. 3b a typical trajectory, particle angle φ as function of time, in this regime for the parameters $\mu = 0.665$ and $\Omega = 43$ Hz. After undergoing oscillations with different amplitudes initially, the particle reaches the centrifugal regime for $t > 1.7$ s. (III) for values of $\mu \gtrsim 0.7$ the particle will reach the centrifugal regime within the first external rotation.

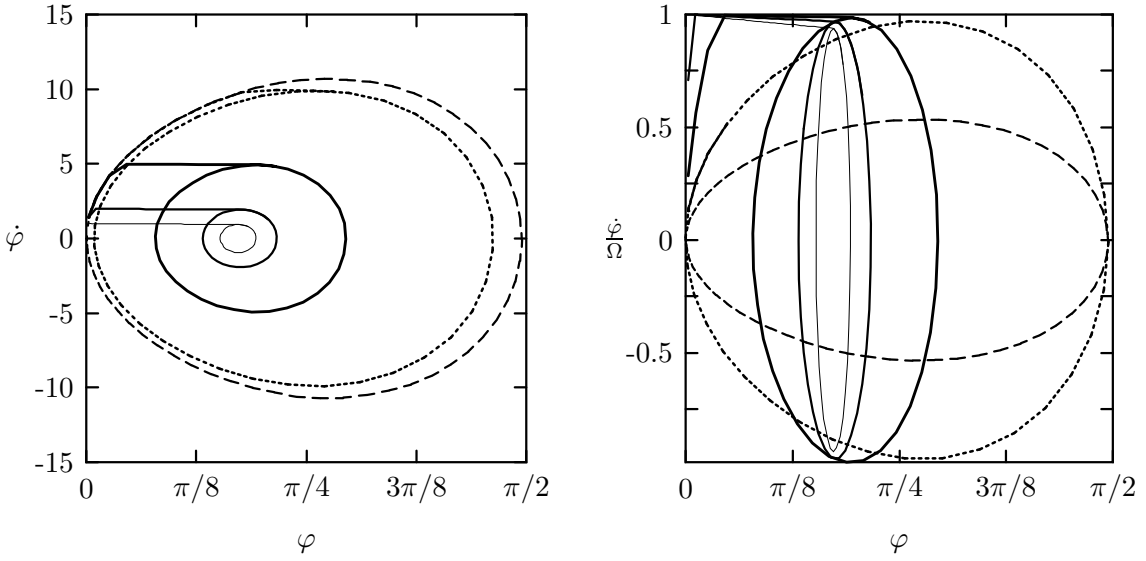


Figure 4: Phase space plot for different angular frequencies $\Omega=1$ (—), 2 (—), 5 (—), 11 (\cdots), 20 (- -) Hz, (a) unnormalized and (b) normalized by Ω .

The transition frequency is independent of the friction coefficient in this regime.

The particle dynamics can be understood in more detail by looking at the motion in phase space, $(\varphi, \dot{\varphi})$, see also ref. [12]. This is shown in Fig. 4 for different rotation speeds, Ω , of the drum, ranging from 1 to 20 Hz and a particle starting initially at $(\varphi, \dot{\varphi}) = (0, 0)$. To the left, Fig. 4a, the motion in the variable $\dot{\varphi}$ is shown whereas to the right, Fig. 4b, $\dot{\varphi}$ is made dimensionless by dividing by Ω . For small values of Ω , the particle initially sticks to the surface and rotates with the constant value $\dot{\varphi} = \Omega$, leading to a horizontal line in phase space. For higher values of Ω , a longer and longer transition period is visible and for the highest value, $\Omega = 20$ Hz, the particle never reaches the value $\dot{\varphi} = \Omega$ but stays in full-sliding motion all the time. After the transition period, the particle oscillates around the value $\varphi = \arctan(\mu_w)$ which shows up as circular motion around the point $(\varphi, \dot{\varphi}) = (\arctan(\mu_w), 0)$ in the phase space plots. For our initial conditions, the maximum extend of the circular regime will be $\varphi \in [0^\circ, 90^\circ]$ and $\dot{\varphi} \in [-\Omega, \Omega]$ which is roughly given by the line corresponding to $\Omega = 11$ Hz in Fig. 4. Please note that the centrifugal motion will correspond to a horizontal line at $\dot{\varphi} \equiv \Omega$.

As discussed above, a simple regularized Coulomb friction law, see Eq. (8), led to two different kinds of trajectories depending on the initial condition of the system. For initial amplitudes below $\Delta\varphi$, the system will oscillate with this amplitude whereas for initial amplitudes above $\Delta\varphi$, the system dissipates energy to reach a final oscillation with an amplitude lower than or equal to $\Delta\varphi$. By considering different friction laws, e.g. choosing a different friction coefficient for the low and high velocity regime, up to four

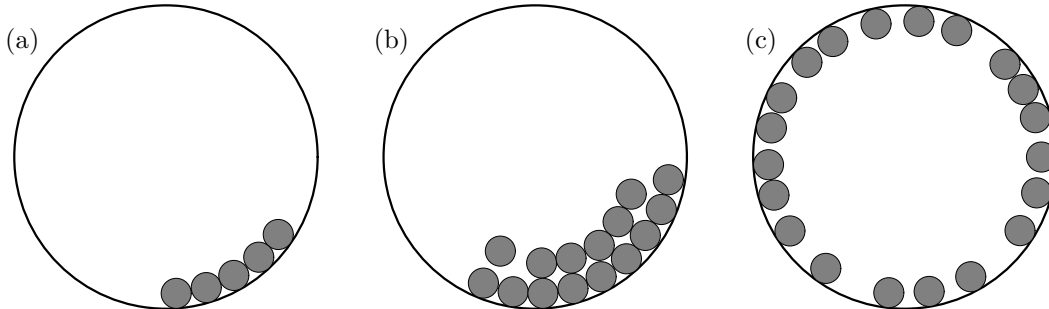


Figure 5: Different motion of few rotating particles N for $\Omega = 50$ Hz, $\mu = 0.75$ and $\mu_w = 0.35$: (a) $N = 5$, (b) $N = 15$ and (c) $N = 20$.

different kinds of trajectories were found analytically [12]. The authors could also partly account for the stick-slip motion and achieved a closer agreement between theory and experiment.

When a round particle, e.g. a sphere, is put in a rotating drum, it will start to rotate with the same sense of rotation as the drum and one might expect to be able to measure indirectly the coefficient of rolling friction by a similar method as described above. Unfortunately, the surface properties in our numerical model are too smooth and the angle of the particle, measured with respect to the vertical, will always give a value around zero, regardless of the angular velocity of the drum or the friction coefficient.

5 Few Rotating Particles in a Two-Dimensional Drum

If more than one round particle is placed in a two-dimensional rotating drum, the particle rotations can be frustrated, i.e. suppressed, whenever particles have more than one contact point. The collective behaviour of all particles will then be very similar to that of a non-rotating particle as described in section 2 and the agreement becomes better with increasing particle number.

To investigate the transition to the centrifugal motion in this case, a two-dimensional MD code is used which includes particle rotations. For the normal forces, the linear force with a linear damping was used and for the tangential force, the viscous friction law with a high enough parameter γ_s , to ensure that mostly the Coulomb friction law applies, was chosen. Two different friction coefficients will be used, namely: i) one for particle-particle collisions denoted by μ and ii) one for particle-wall collisions denoted by μ_w which will be varied independently. All particles have a diameter of $d = 1$ cm and the drum diameter was $D = 10$ cm. This gives a maximum of 28 particles that can form

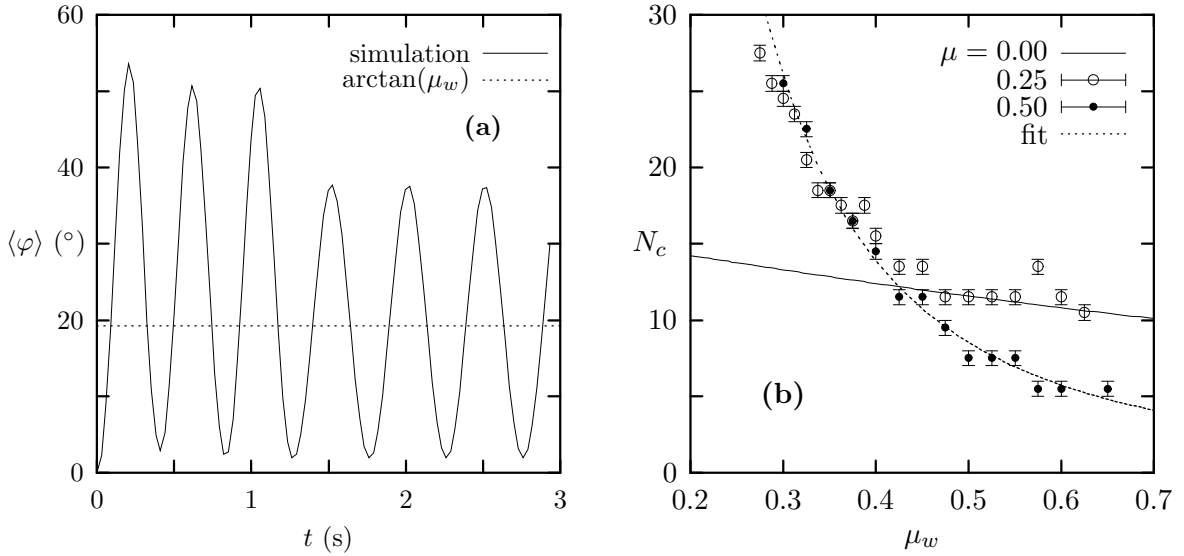


Figure 6: (a) Average angle of 5 rotating particles for $\Omega = 50$ Hz, $\mu = 0.75$ and $\mu_w = 0.35$ and (b) critical particle number for the transition to the centrifugal regime as function of wall friction for three different particle-particle friction coefficients μ . The theoretical curve corresponds to the case $\mu = 0.00$.

the outer ring in the centrifugal regime and we limit our investigations to this value in order for all particles to feel the wall friction.

For only a few number of particles, they will all form a line, shown in Fig. 5a for $N = 5$, and the motion will essentially be one-dimensional. For more particles, where the exact number depends linearly on the drum to particle diameter ratio, D/d , more than one layer or ring of particles will form, shown in Fig. 5b for $N = 15$, and the motion is no longer one-dimensional but two-dimensional. Above a critical particle number, N_c , which depends on D/d as well but also on the friction coefficient, μ , all particles will form a single ring again but make full overturns [13]. Such a situation is depicted in Fig. 5c for $N = 20$ and will be called the *centrifugal regime* in this case.

First we look at the angle with respect to the vertical averaged over all particles, $\langle \varphi \rangle$, as a function of time. For a small number of particles, it shows a similar behaviour as the angle of a non-rotating particle which is shown in Fig. 6a for the configuration from Fig. 5a. Initially, the five particles form two layers but reorganize into one layer at $t \approx 1.25$ s which can be seen in Fig. 6a by the change in amplitude. After this reorganization, oscillations around $\arctan(\mu_w)$, shown as dotted line, will occur as was the case for one non-rotating particle, see Fig. 1b.

To investigate the parameter regimes of the different motions depicted in Fig. 5, especially the transition to the centrifugal regime, we determine the minimal number of

particles, N_c , which are necessary to reach it. For an inter-particle friction coefficient of $\mu = 0.0$, all particles will form a single ring since piles cannot be supported. The particle configuration will fluctuate around a mean angle of $\langle\varphi\rangle = \arctan(\mu_w)$, see Fig. 6a. As discussed in the preceding section, a necessary condition for overturns is that the center of mass of the top-most particle reaches an angle of more than $\frac{\pi}{2}$. The angle φ is measured from the vertical pointing downwards again, as shown in Fig. 1a. Assuming that all particles are forming a single block and are touching their neighbours, the center of mass of the top-most particle of a configuration of N particles is at an angle of $\arctan(\mu_w) + \frac{d}{D}(N - \frac{1}{2})$. This gives as necessary condition for overturns

$$\arctan(\mu_w) + \frac{d}{D}(N - \frac{1}{2}) > \frac{\pi}{2}$$

which when solved for the critical particle number, N_c , gives

$$N_c > \frac{D}{d}(\frac{\pi}{2} - \arctan(\mu_w)) + \frac{1}{2}. \quad (10)$$

This analytic expression for N_c , derived for an inter-particle friction coefficient of $\mu = 0.0$, is shown in Fig. 6b as function of the wall friction coefficient, μ_w , as solid line. Also shown are the numerical results for $\mu = 0.25$ (\circ) and $\mu = 0.50$ (\bullet) with a dotted line as least-square power law fit to the data points for the latter case to guide the eye. The differences with the analytic curve can be explained in the following way: If the inter-particle friction is sufficiently high, already two rotating particles can behave as a non-rotating particle in the two-dimensional drum. From the preceding section, one recalls that overturns are possible for one non-rotating particle if $\mu_w \gtrsim 0.65$. Therefore, the critical particle number will *decrease* with increasing inter-particle friction for a high wall friction coefficient and we get $\lim_{\mu \rightarrow 1} N_c = 2$ for $\mu_w \gtrsim 0.65$. This is in perfect agreement with the numerical data where the data points for $\mu = 0.25$ lie very close to the analytic curve for $\mu_w > 0.45$ and N_c decreases with increasing μ giving a value of $N_c \approx 5$ for $\mu = 0.5$ and $\mu_w = 0.65$.

For low wall friction coefficients, a larger number of particles is needed to reach the centrifugal regime since the value of $\arctan(\mu_w)$ is small. If $\mu > 0$, the particles can be arranged in more than one layer which gives a lower height for the top-most particle as compared to the one layer case discussed above. Consequently, N_c will *increase* with increasing inter-particle friction for a low wall friction coefficient since the layer structure becomes more stable which is supported by the numerical data.

6 Conclusions

We investigated analytically the motion of a non-rotating particle in a rotating drum in the full-sliding limit. The angle of the particle's center of mass oscillates around a

mean value, given by the particle-wall Coulomb friction coefficient. The one-dimensional description breaks down for angles above 90° , corresponding to free flights of the particle. In order to study the full dynamics, including the transition from sticking to sliding motion for low velocities of the contact surfaces, we simulated the system using molecular dynamics. Full agreement with the analytic results in the full-sliding case was achieved and the general trend of the frequency dependence of the average particle angle observed in experiments could also be reproduced. The phase diagram of the transition to the centrifugal motion revealed three different regimes.

We also found that the collective motion of a few rotating spheres in a two-dimensional rotating drum is, to a certain extent, similar to the motion of one non-rotating particle in a drum due to the frustrated particle rotations. We derived an analytic expression for the minimal number of particles to obtain centrifugal motion in the limit of negligible inter-particle friction. It compares well with the experimental findings and the change when inter-particle friction is added can be understood as well.

Acknowledgments

We gratefully acknowledge fruitful and helpful discussions with C. Dury, A. Betat, K. Kassner, I. Rehberg and A. Schinner. Special thanks go to M. Scherer for sharing his experimental ideas with us and to the *Deutsche Forschungsgemeinschaft* for financial support.

References

- [1] H. M. Jaeger, S. R. Nagel, and R. P. Behringer, *Physics Today* **4**, 32 (1996).
- [2] J. Rajchenbach, *Phys. Rev. Lett.* **65**, 2221 (1990).
- [3] C. M. Dury, G. H. Ristow, J. L. Moss, and M. Nakagawa, *Phys. Rev. E* **57**, 4491 (1998).
- [4] N. Nityanand, B. Manley, and H. Henein, *Metall. Trans. B* **17**, 247 (1986).
- [5] M. Caponeri, S. Douady, S. Fauve, and C. Laroche, in *Mobile Particulate Systems*, edited by E. Guazzelli and L. Oger (Kluwer, Dordrecht, 1995), p. 331.
- [6] B. Bhushan, J. N. Israelachvill, and U. Landman, *Nature* **374**, 607 (1995).
- [7] F. Heslot, T. Baumberger, B. Perrin, B. Caroli, and C. Caroli, *Phys. Rev. E* **49**, 4973 (1994).

- [8] F.-J. Elmer, *J. Phys. A: Math. Gen.* **30**, 6057 (1997).
- [9] A. Betat and I. Rehberg, in *Friction, Arching, Contact Dynamics*, edited by D. E. Wolf and P. Grassberger (World Scientific, Singapore, 1997), p. 301.
- [10] K. Kassner, private communications, 1996.
- [11] G. H. Ristow, in *Annual Reviews of Computational Physics I*, edited by D. Stauffer (World Scientific, Singapore, 1994), p. 275.
- [12] A. Schinner and K. Kassner, in *Friction, Arching, Contact Dynamics*, edited by D. E. Wolf and P. Grassberger (World Scientific, Singapore, 1997), p. 305.
- [13] M. Scherer, private communications, 1996.

